Arab Institute of Navigation
Cross Road of Sebaei Street& 45 St.,
Miami, Alexandria, Egypt
Tel: (+203) 5509824
Cell: (+2) 01001610185
Fax: (+203) 5509686
E-mail: ain@aast.edu
Website: www.ainegypt.org

Journal of
The Arab Institute of Navigation

Semi Annual Scientific Journal
Issue 46 (volume 2) July 2023
pISSN (2090-8202) - eISSN (2974-4768)
https://doi.org/10.59660/46772
INDEXED IN (EBSCO)

Contents

Numerical analysis of the buoy design to extract the effective kinetic wave energy.

Prepared By
Mohamed Walid Abd Elhamed Ahmed Refae [(1)i], Ahmed S. Shehata [(2)] and Mohamed Abass Kotb [(3)]
Arab Academy for Science, Technology and Maritime Transport, Egypt

DOI NO. https://doi.org/10.59660/467313
Received 06 April 2023, Revised 07 May 2023, Acceptance 20 June 2023, Available online and Published 01/07/2023

المستخلص

في العديد من البلدان، أصبحت طاقة أمواج البحر معترف بها على نطاق واسع كمورد هام ومفعم بالأمل. الهدف من هذا البحث هو تقييم تأثير التعديلات في شكل العوامة على فعالية نموذج الموجة من خلال استخدام ديناميكيات السوائل الحاسوبية (CFD) لتقييم التعديلات في السلوك الديناميكي للعوامة. يتم محاكاة سلوك العوامة باستخدام برنامج ANSYS Fluent، وقياس حجم اقتراب السوائل ، ووحدة تدفق خلال سير السوائل، وتطبيق نماذج موجة Stokes من الدرجة الخامسة. لمزيد من التحقيق في حساسية الموجة في الظروف الصعبة، تم تطبيق موجات ستوكس في المجال الضحل عند انحدار الموجة العالية .تتكون عملية التحقق من تحليل مقارن بين النتائج العملية والرياضية. تمت مقارنة نتائج الحساب الديناميكي للسائل العددي، وتم تعديل الملاحظات المختبرية. للتكوينات المختلفة للطفو تحت الماء، تم تحليل خصائص السحب والرفع للنتائج العددية. الهدف من هذه الدراسة هو التعرف على الشكل الأمثل للعوامات. استند اختيار هذا الشكل إلى عدة عوامل، كان أهمها أقل إنتروبيا، بالإضافة إلى الحد الأقصى لمعامل الرفع والسحب. تم تحديد الشكل المثالي ليكون كروي الشكل (الشكل ب).

1. Abstract

In many countries, sea wave energy is becoming more widely recognized as a significant and hopeful resource. The objective of this research is to evaluate the impact of alterations in buoy shape on the efficacy of the wave model by utilizing Computational Fluid Dynamics (CFD) to assess modifications in the buoy's dynamic behavior. The buoy's behavior is simulated using ANSYS Fluent, the volume of fluid approach, the open channel flow module, and 5th order Stokes wave models. To further investigate the wave sensitivity in challenging circumstances, Stokes waves were applied in the shallow domain at high wave steepness. The validation process consisted of a comparative analysis between the practical and mathematical results. The outcomes of a numerical fluid dynamical computation were compared, and laboratory observations were modified. For various configurations of underwater buoyancy, the drag and lift characteristics of numerical results were analyzed. The aim of this study was to identify the optimum buoy shape. The selection of this shape was based on several factors, of which the most significant were the least entropy, as well as the maximum lift and drag coefficient. Ideal shape was determined to be a spherical shape (shape B).

2. Introduction

The energy crisis and environmental degradation have gotten worse recently as a result of traditional energy sources' unreliability and detrimental effects on our daily life. Due to their sustainability and environmental friendliness, renewable energies like solar, wind, and ocean energy have thus been employed as an alternative to conventional energy (Jacobson, 2015). Studies have shown that ocean waves are denser than the sun and wind (Falnes, 2007). Around 2-terawatt worth of wave energy is commercially viable, which is sufficient to provide the entire world's energy needs in 2008(Gunn, 2012). GIRARDS created the first wave energy device in 1799 (Falcão, 2010). Three categories of wave energy converters—point absorbers, attenuators, and terminator—can be distinguished (Drew, 2016). One of the finest choices for ocean devices in the wave energy sectors is the floating point absorber (B. Lei, 2017). The majority of the time, forces between two bodies act to extract wave energy from wave energy converters (Viet,2016). Flexible polyvinylidene fluoride (PVDF) was used by Taylor et al. to (2001) develop an eel-like device that transforms mechanical energy from flowing river or ocean water. By leaving a predictable path of travelling vortices, the device stresses the piezoelectric components for the generation of electrical power (George, 2001). Optimisation should lower manufacturing costs for the majority of wave energy converter (WEC) systems currently in the precommercial stage. The progress and responsiveness of the launch mechanism, particularly the travel of the buoy across a predetermined route, have an impact on the WEC's efficiency (Aderinto, 2019). According to Viet, (2016) for the converters to successfully absorb energy, absorber floats are required. The buoy's size, shape, and wave incidence features affect how it moves in waves. In a separate experiment, Pastor (2014) looked at the behavior of different buoys during the same wave excitations to maximize the energy. Although their masses varied, the identical twin boys had the same radius. In their study, Amiri and Radfar examined how well four buoy versions with various radii and the same mass absorbed wave energy (Amiri, 2016). De Backer (2010) used a separate method to determine the mass of the buoys. According to its mass, the amount of water it is in, the gravitational force it is subjected to, and its hydrodynamic properties, the floating body moves according to the motion equations of the drifting body. Due to the variations in the ambient conditions, wave height characteristics, and buoy sizes, it is difficult to compare the researcher's results. Giorgi (2016) discovered that cylindrical buoys had significantly higher simulation forces than spherical buoys (Giorgi, 2016). The buoys were the same size and depth. Lopez (2017) study buoys in both periodic and erratic waves. The forms of the floating component were cylindrical, reversed conical, and had slightly bent ends. In order to increase productivity, it had a spherical underwater body. Mahdi (2019) investigated several diameters and droughts for the region of Rio de Janeiro. By relating experimental findings to RAWs based on simulation and the energy intake of a cylindrical-hemispherical buoy (Mahdi ,2019). Hulme (1981) created the swinging instrument using his knowledge of how water molecules move in waves. The device's capture width ratio was raised by improving the pendulum WEC. Wave energy is made up of kinetic and potential energy. The buoy's hydrodynamic efficiency will be improved if its heaving and pitching motions are used effectively (Hulme, 1981). Models must be evaluated to fully understand the fluid/structure relationship that affects the offshore construction. Unavoidably, testing will take place in a small

scale in the lab before being done in real seawater. However, the development of simulation programs has made it easier to do quick research. That is, if the mathematical model utilized accurately simulates the actual environment. (Finnegan, 2012). Numerical wave tanks (NWTs) are the names given to the numerical models that imitate wave tanks. Numerous numerical techniques are used to build NWTs. A wave is created in a NWT at the input border and is dampened close to the output limit. Kim et al., (2001) mathematically simulated 3-D nonlinear waves with several directions that use the fixed-difference approach. Using a numerical wave maker, the waves were produced by setting the speed of water molecules to the wave maker limits (Kim et al, 2001) To investigate the impact of an irregular waveform, Koo and Kim (2004) enhanced the procedure to incorporate fluid structure interactions (Koo and Kim, 2004) .Sun and Faltinsen (2006) modeled a two-dimensional simulated bowl to model the effects of buoy on an open surface (Sun and Faltinsen, 2006) .An irregular wave bowl was modeled using complex equations by (Ning et al,2007). YOU and LIU (2011) modeled irregular wave behavior. As an example of wave-body interaction, they looked at fluid motion inside a sphere (YOU and LIU ,2011). Wu and Hu (2004) simulated the unsteady relationship among water and buoys mathematically (Wu and Hu, 2004). Angeliki (2023) has studied that the buoy's dynamic behavior, ability to absorb energy, and capacity to convert wave kinetic energy into direct and indirect electrical energy depend gently on the shape and the material selection (Angeliki, 2023). Jessice's (2022) investigation includes an analysis of wave energy's current state development, methods and technology for utilizing it, effects on the environment and benefits and drawbacks of using it (Jessice's,2022). Studies comparing forces on the fixed structure to the measurement of the free surface height are likewise limited, particularly in the shallows. When constructed to the costly experimental setup, the CFD would be a more realistic output. To further explore the effect of wave shape on wave energy devices, ANSYS Fluent was used in this article to perform CFD analysis. This analysis allowed researchers to investigate how waves interact with structures and how arrays of different types of devices are affected by the waves. The study compared numerical findings to experiments and reviewed the validation method used for accuracy. The results of this research were applied to various underwater buoys to determine the effectiveness of different wave energy devices. Additionally, this research has opened up the possibility for further development in wave energy technologies, as well as other potential applications for CFD analysis.

3. Methodology

The creation of numerical models and running of simulations were done using ANSYS Fluent. By contrasting the numerical results with those from the trials by obtaining the free surface level at two locations in the wave tank with the same parameters as Bhinder's (2009) simulation of the wave tank was approved before modelling the point absorber. After validation, altering buoy's shape signaled the beginning of the wave simulation of the point absorber. The dimensions were utilized to calculate the lift and drag coefficients in the second stage of the simulation. Conical, spherical, and other buoy shapes are considered. Pressure, velocity magnitude, entropy and lift and drag coefficients were computed. To get the most energy and experience the fewest losses, the optimum design was chosen.

3.1 Validation

The validation process was separated to 3 phases:

(1) The geometry, which dictated the model's actual size.

(2) The mesh configuration, which was created and refined to measure the free surface height.

(3) The physical setup, which determined the evaluation, region configuration, water depth, and other fluids interaction characteristics.

3.1.1 Geometry Setup

The wave tank that was used for the experimental study was 35 m, 2.5 m, and 1.5 m. The tank was equipped with multi-element regular 2D wave generation equipment. The tank was designed considering the wave-damping zone to minimize the reflection. The tank was filled was one fluid, its properties are shown in Table (1).

Table 1: properties of fluid

K (W/m. K)	0.597
ρ (kg/m3)	1000
T (°C)	20
Q (J/kg. K)	4182
μ (kg/m. s)	0.001

Waves can be formed in diverse ways resulting in waves with different characteristics, different heights, lengths, and periods Fig (1). These variables must be determined in for the complicated sea state to be characterized by the energy spectrum. The wave characteristics are shown in Table (2)

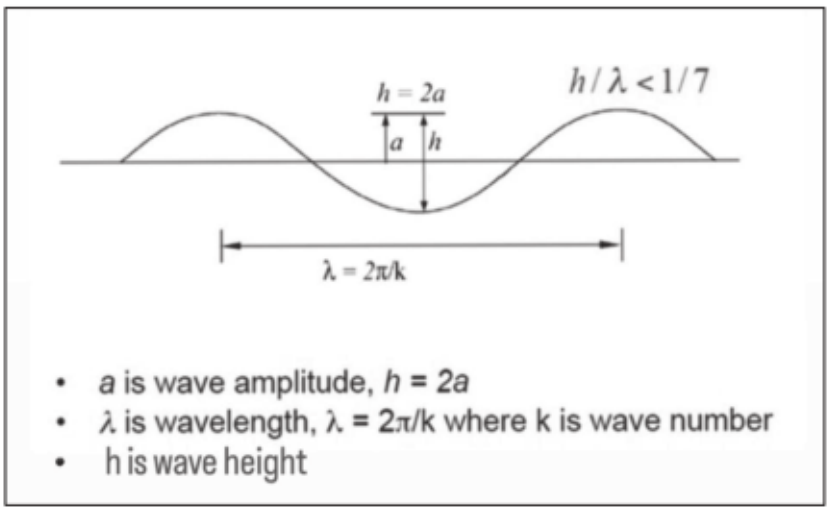

Fig (1) Wave Characteristics

Table 2: wave value

Wave height	0.3m
Period Time	4.2s
Water Depth	1.5m

3.1.2 Mesh Setup

Mesh generation is a critical component of computational fluid dynamic modeling. The domain is shown in Fig (2). The mesh structure was modified to reduce the problem time significantly. Different mesh configurations were tested and the optimum mesh was selected (Bhinder et al., 2009). The size of mesh was 600000 and the size function was selected to be curvature as illustrated in Fig (3).

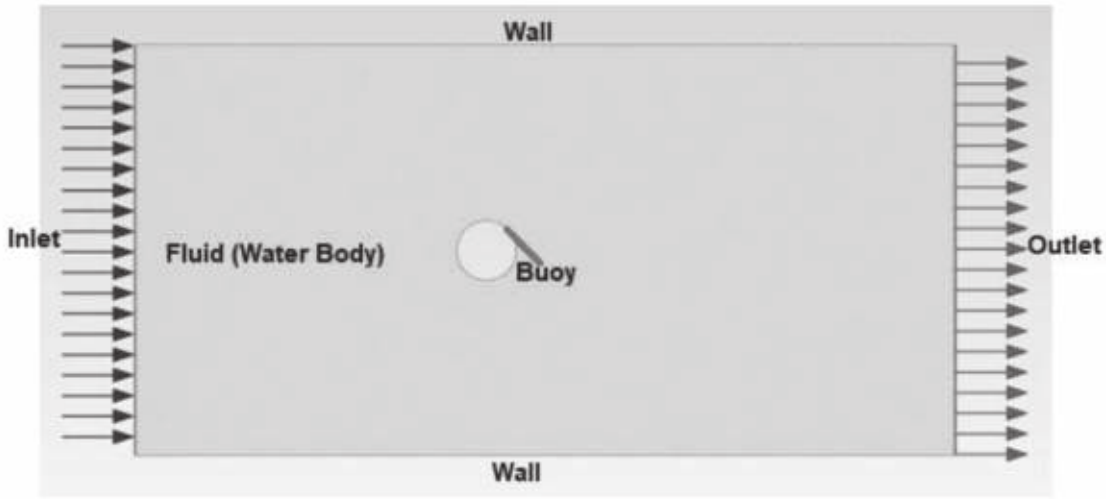

Fig (2) Fluid Domain

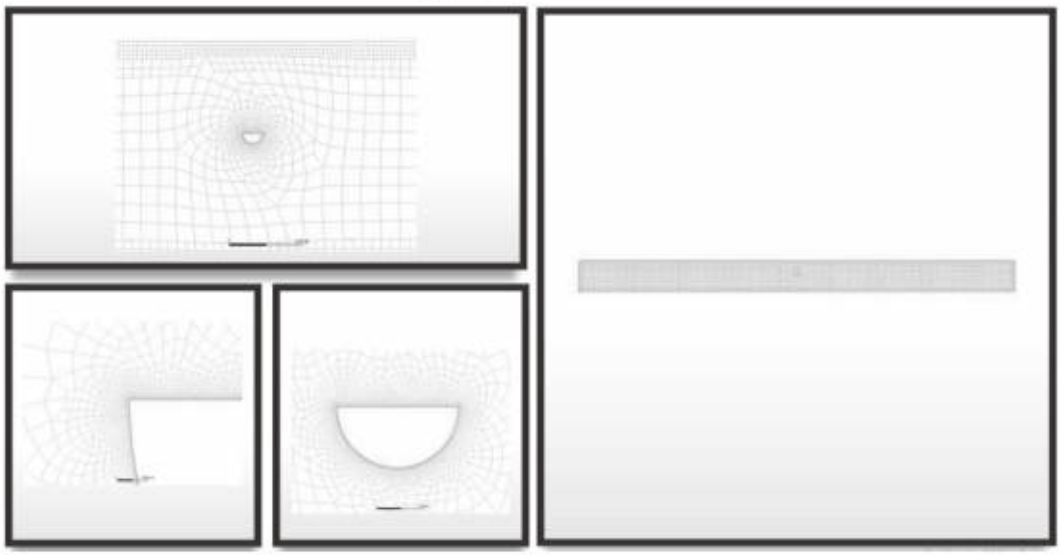

Fig (3) Mesh Structure in the Wave Tank

3.1.3 Physics Setup

The finite volume technique is the strategy used in ANSYS Fluent to solve the problem. The target region is divided into smaller regions by using this technique. The simulation was carried out while second-order monotonicity-preserving momentum and continuity equations were iteratively solved across each sub-region. As a result, an approximate value for each variable is obtained at various places within the domain (Malalasekera et al., 2007).

One of the equations that can be simulated by ANSYS is represented as,

$$\frac{\partial p}{\partial t} + \frac{\partial p u_1}{\partial x} + \frac{\partial p u_2}{\partial y} = 0 \quad (1)$$

And Navier-stokes equations, which are given as,

$$p\left(\frac{\partial u_1}{\partial t} + u\frac{\partial u_1}{\partial x} + v\frac{\partial u_1}{\partial y} = -\frac{\partial p}{\partial x} + 2\mu\frac{\partial^2 u_1}{\partial x^2} + \frac{\partial}{\partial y}\left(\mu\left(\frac{\partial u_1}{\partial y} + \frac{\partial u_2}{\partial x}\right)\right) + F_1 \quad (2)$$

$$p\left(\frac{\partial u_2}{\partial t} + u\frac{\partial u_2}{\partial x} + v\frac{\partial u_2}{\partial y} = -\frac{\partial p}{\partial y} + 2\mu\frac{\partial^2 u_2}{\partial y^2} + \frac{\partial}{\partial x}\left(\mu\left(\frac{\partial u_1}{\partial y} + \frac{\partial u_2}{\partial x}\right)\right) - pg + F_2 \quad (3)$$

Where,

p	*Pressure*	t	*Time*	x	*Horizontal Distance*
u_1	*Horizontal Flow Velocity*	u_2	*Vertical Flow Velocity*	y	Vertical Height
F_1	*Horizontal Force*	F_2	*Vertical Force*	μ	*Viscosity*

Since the RNG turbulence model was extremely precise and dependable provided by the software, it was used for all simulations. Swirling's impact on turbulence in the RNG model, clarity in whirling flows.

$$\frac{\partial}{\partial t}(pk) + \frac{\partial k}{\partial x_i}(pku_i) = \frac{\partial}{\partial x_j}\left[(\alpha_k u_{\varepsilon ff})\frac{\partial k}{\partial x_i}\right] + G_k - \rho\varepsilon \quad (4)$$

$$\frac{\partial}{\partial t}(p\varepsilon) + \frac{\partial k}{\partial x_i}(p\varepsilon u_i) = \frac{\partial}{\partial x_j}\left[(\alpha_\varepsilon u_{\varepsilon ff})\frac{\partial \varepsilon}{\partial x_i}\right] + G_{l\varepsilon}\frac{\varepsilon}{k}G_k - G^* G^*_{2\varepsilon\rho}\frac{\varepsilon^2}{k} \quad (5)$$

$$G^*_{2\varepsilon} = G_{2\varepsilon} + \frac{c\mu\rho\eta^3(1-\frac{\eta}{\eta_O})}{1+\beta\eta^3} \quad (6)$$

$$\eta = \frac{sk}{\varepsilon} \quad (7)$$

Where,

G_k	*Kinetic Energy Generation*
G_{21} $G_{2\varepsilon}$	*Model Constants*
k	*Turbulence Kinetic Energy*
ε	*Rate Of Dissipation.*

An explicit solution differed from an implicit solution in that an explicit solution was solved gradually by stepping through time at each computing cell, but the time step in an implicit solution was confined to fulfil requirement for stability. However, using information from a previous time step, an implicit solution was solved in each timestep, which calls for more intricate iterations without imposing time step restrictions.

The Split Lagrangian approach was utilized in the Numeric tab's volume of fluids (VOF) addictive section because it produced lower cumulative volute error than other methods provided by ANSYS Fluent.

The boundary conditions are illustrated in Fig (4). The model was developed using fifth-order Stokes wave theory (Bhinder et al., 2009) based on the specifications of the simulated wave.

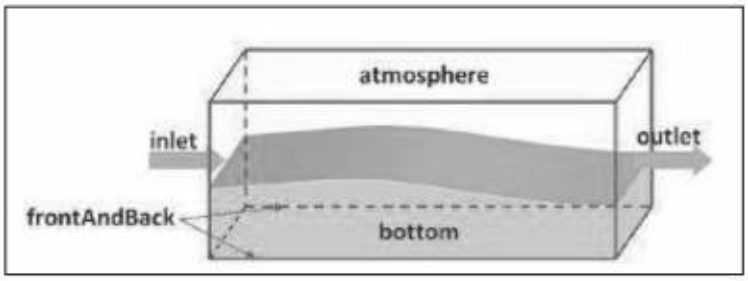

Fig (4) Boundary Conditions

The Fluent segregated solver was applied in these computations. It takes several rounds of solution loops before convergence is attained because the governing equations are nonlinear. The schemes were referred to as the pressure-based segregated algorithm as PISO was recommended for transient calculations.

3.2 Buoy Modelling

This study recommends creating a similar setting in to compare the behaviors of several buoys in waves. There are four different types of buoy shapes considered; conical and spherical, and odd buoys. Fig (5). To understand The results of these adjustments on the effectiveness of the wave energy model, the CFD is used to assess changes in the buoy's hydrodynamic characteristics brought on by changes in buoy shape. The radius chosen in this study, 0.1 m was simulated to determine the drag and lift coefficients.

$$F_X = \frac{1}{2}\rho C_{DX} D u \sqrt{(u^2 + w^2)} + \rho C_{MX} A \dot{u} \quad (8)$$

$$F_y = \frac{1}{2}\rho C_{DY} B w \sqrt{(u^2 + w^2)} + \rho C_{MY} A \dot{w} \quad (9)$$

Where,

F_X	Horizontal Force	C_{DX}	Horizontal Drag Coefficient
D	Depth	u	Horizontal Velocity
ρ	Denisty	C_{MX}	Horizontal Inertia Coefficient
A	Area	$\dot{u}$	Horizontal Acceleration
F_y	Vertical Force	C_{DY}	Vertical Drag Coefficient
B	Width	w	Vertical Velocity
C_{MY}	Vertical Inertia Coefficient	$\dot{w}$	Vertical Acceleration

Entropy minimization is the primary branch in the design of energy systems. It is the most efficient method of calculating missing energy and work destruction. As a result, much attention has been focused on the topic of entropy development due to heat and mass transmission. Strain-originated breakdown and thermal loss, which represent the creastion of viscous and thermal entropy, respectively, are the two factors in fluid flow (Iandoli, 2005). The creation of entropy can be represented as (Shehata, 2016).

$$S_{gen} = S_V + S_{th} \quad (10)$$

The local viscous irreversibiliities is expressed as,

$$S_V = \frac{\mu}{T_o} \emptyset \quad (11)$$

$\emptyset$ -- the viscous dissipation term that can be written as,

$$\emptyset = [(\frac{\partial u}{\partial x})^2 + (\frac{\partial v}{\partial y})^2] + (\frac{\partial u}{\partial y} + \frac{\partial v}{\partial x})^2 \quad (12)$$

So the entropy generation can be expressed as:

$$S_G = \iint S_V dy dx \quad (13)$$

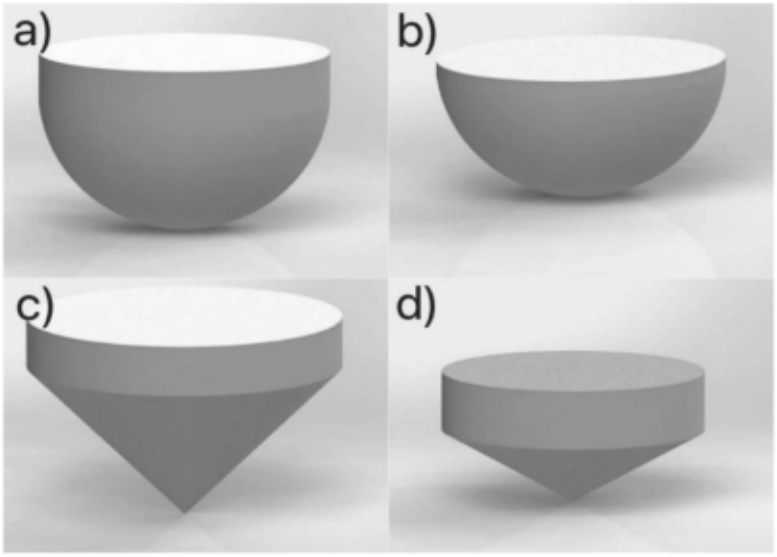

Fig (5) Buoy Shapes

4. Results and discussion

For Euler equations as well as additional scalars like turbulence, the integral equations were fluidly solved. Using a computational grid and a control volume-based approach, the domain was split into discrete volume controlled. The governing equations were included into the structure to produce mathematical formulation for small variables.

4.1 Validation

A linear wave was modeled using the same parameters as Bhinders et al., (2009) study to produce a relation between free surface height and the number of seconds, which the three highest peak values from each case were compared, it was discovered that the difference was less than 10 %, Table (3). This small discrepancy results from other settings which were not mentioned clearly in the study.

Table (3) difference of results for surface elevations bet model & simulation

Distance (m)	Highest `peak	Free surface elevation from the baseline model	Free surface elevation from simulation results
2.1	First Peak	0.18	0.17
	Second Peak	0.19	0.18
	Third Peak	0.185	0.175
6.5	First Peak	0.155	0.155
	Second Peak	0.155	0.145
	Third Peak	0.145	0.14

4.2 Buoy Results

The lift and drag coefficients of the various buoy forms were calculated using a CFD software program (Fluent). Fluid estimates the computer simulation's fluid dynamic properties. Fluid dynamic software was used to create a mesh around the geometrical model of the buoy and start the calculations. After many rounds of iterations, the simulation achieved its conclusion. The result of the simulation depends on the starting boundary conditions, the size of the grid, and the flow conditions estimated at each node in the mesh.

4.2.1 Pressure

The pressure was the first variable studied by fixing the radius and mass of the four buoys. It can be observed that the flow from the inlet moves toward the outlet of the tank. Contours were obtained at each buoy shape and compared to other shapes. A graph was also created to show how pressure changed in the axial direction. The resulting profile is shown in Fig (6), while Fig (7) illustrates the pressure distribution over the distance.

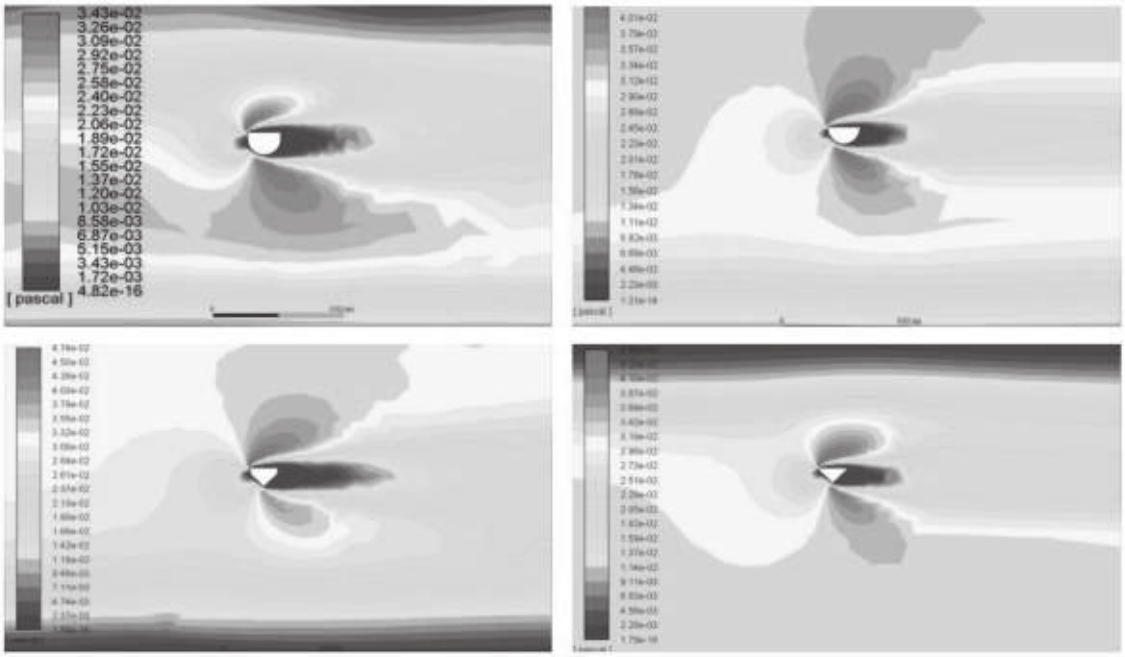

Fig (6) Static Pressure Contour

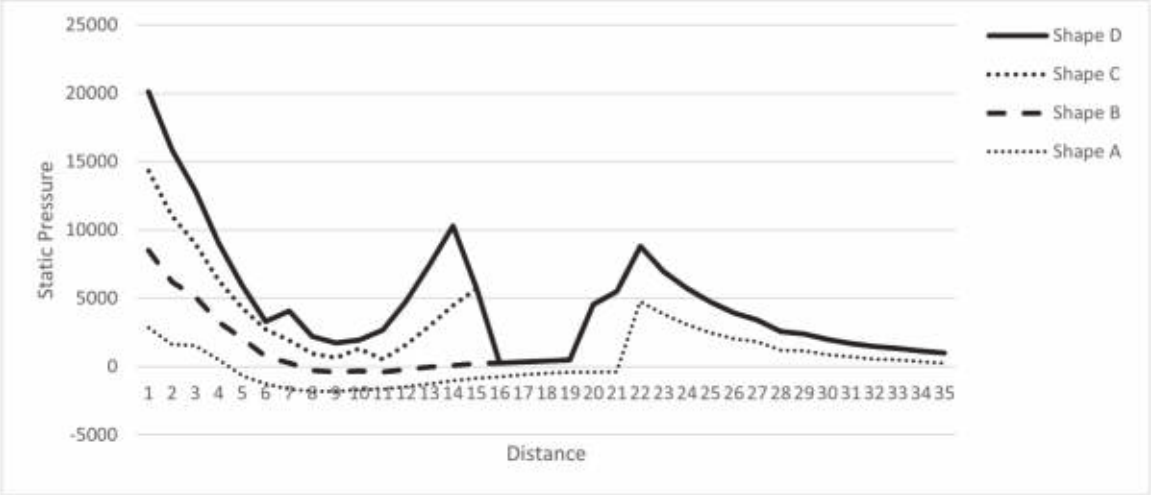

Fig (7) Pressure Distribution

4.2.2 Velocity Magnitude

By keeping the buoy's size and weight constant, the contours illustrate how the buoy's shape affects its average velocity. The average velocity was selected based on the environmental conditions as Bhinder et al., (2009) mentioned. The initialization was computed from the inlet and traveled toward the tank's outlet. It was useful to view the vector and contour plots individually. While the vector plots provided a better indication of the fluid's flow direction as shown in Fig (8), the contours provided a better representation of the velocity magnitude for each buoy shape as shown in Fig (9).

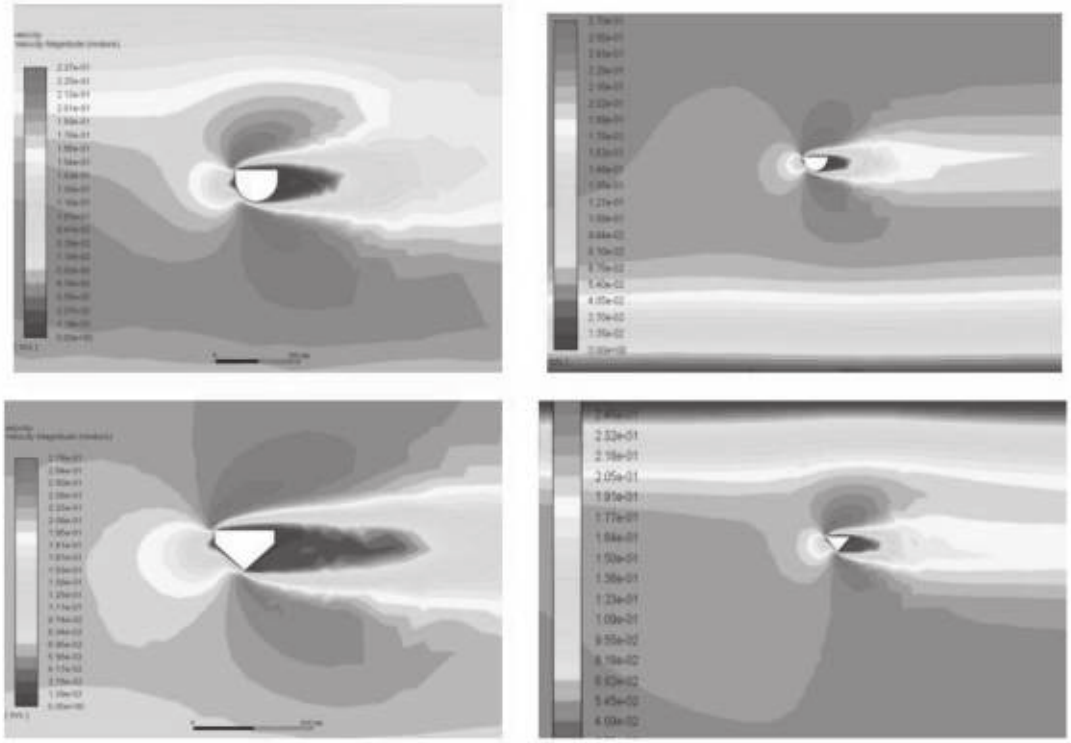

Fig (8) Velocity Contour

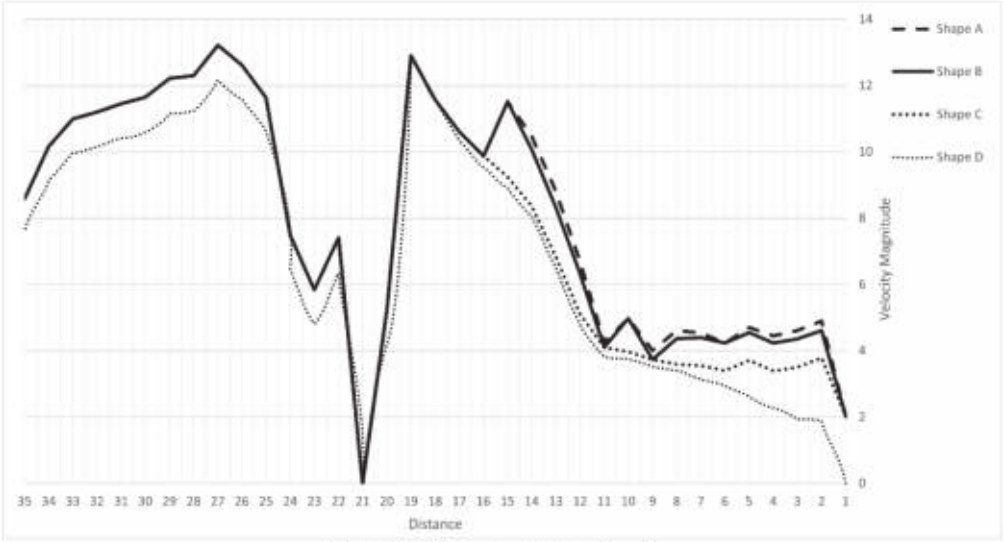

Fig (9) Velocity Distribution

4.2.3 Entropy

Entropy can potentially affect buoys in several ways, depending on the context and specific factors involved like wave action, corrosion, and thermal expansion. Wave action can affect buoys as the movement of water is a manifestation of energy, and the more chaotic the motion, the higher the entropy. Therefore, in areas with high wave energy, buoys may experience more wear and tear due to the increased forces acting on them. Buoys are typically exposed to seawater and atmospheric

conditions, which can lead to corrosion of the buoy's metal components. Corrosion is a naturally occurring process that involves the breaking down of metals into their constituent ions, and it is driven by thermodynamic principles, including entropy. Specifically, corrosion tends to occur in environments where there is a high degree of disorder and randomness, which is reflected in the higher entropy of the system. Moreover, buoy materials are often subject to thermal expansion due to changing temperatures. Thermal expansion is a manifestation of increased molecular activity that occurs at higher temperatures, resulting in an increase in entropy. As a result of this thermal expansion process, buoys can experience changes in shape or size which may have a direct effect on their performance or longevity. Additionally, these changes may cause metal fatigue or other structural stresses that can reduce a buoy's resistance to wave motion or corrosion over time. Overall, entropy can have a range of effects on buoys depending on the specific circumstances and mechanisms involved. However, it is important to note that buoys are designed and engineered to withstand the harsh conditions of the marine environment; factors such as corrosion and thermal expansion are generally considered in their design and maintenance to ensure their longevity and performance over time. Fig (10) shows the evaluation of entropy distribution in the fluid flow direction for the four shapes.

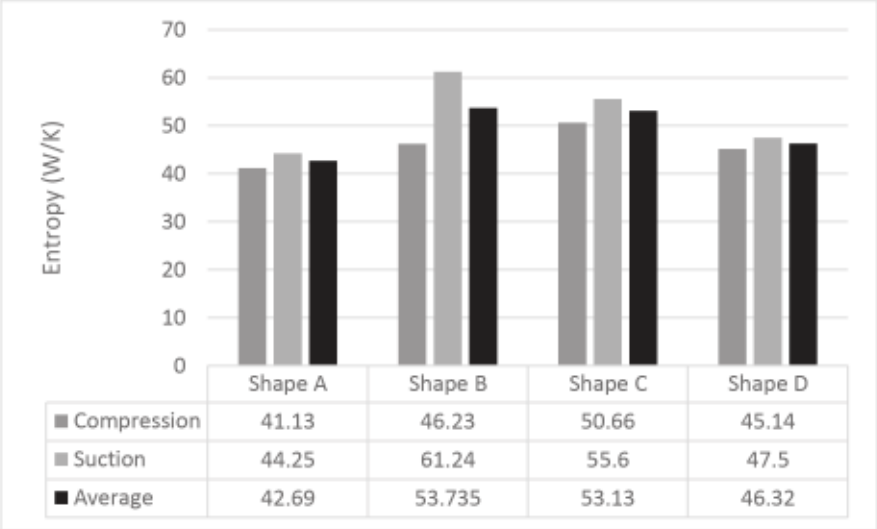

	Shape A	Shape B	Shape C	Shape D
Compression	41.13	46.23	50.66	45.14
Suction	44.25	61.24	55.6	47.5
Average	42.69	53.735	53.13	46.32

Fig (10) Entropy Distribution

4.2.4 Lift Coefficient

The lift force coefficient is affected by the Reynolds number, the amplitude ratio, and the amplitude ratio, and the lowered velocity. The lift coefficient is the factor that engineers use to represent all the complicated dependencies of shape, inclination, and other conditions. The lift coefficient results from the heave and pitch oscillations are presented in Fig (11).

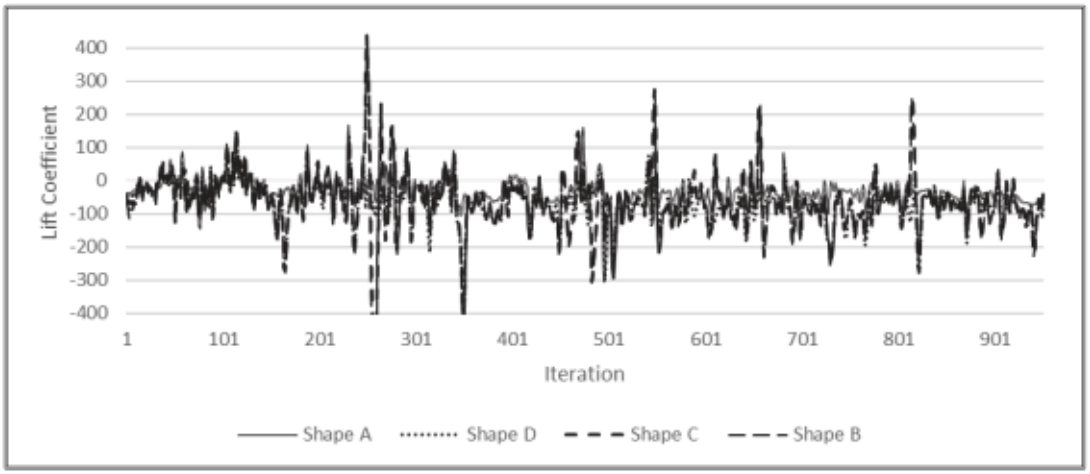

Fig (11) Lift Coefficient

4.2.5 Drag Coefficient

The buoy's shape, the flow's Reynolds number, and the surface's roughness are only a few of the variables that affect the drag coefficient. Along with intricate buoy dependencies, the drag coefficient also takes fluid viscosity and compressibility into account. Figure (12) displays the drag coefficient for four different forms.

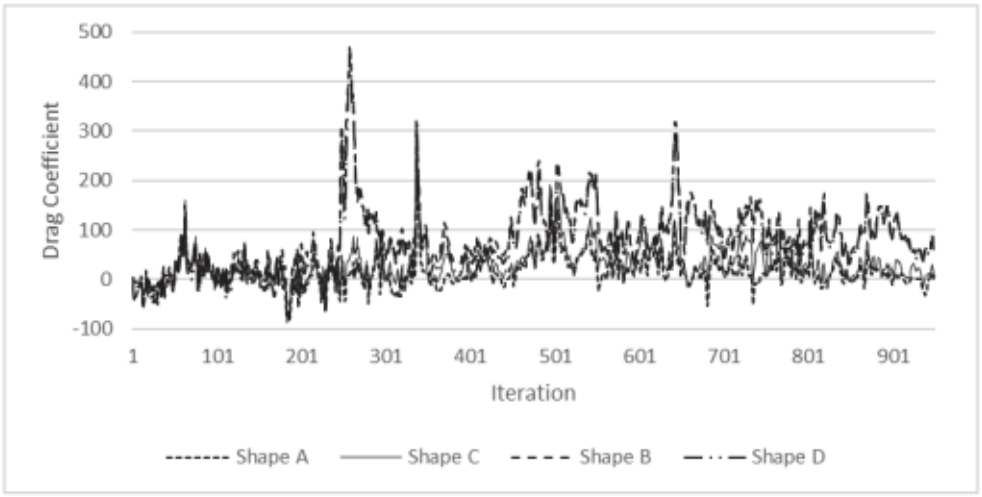

Fig (12) Drag Coefficient

5. Conclusion

In conclusion, the ANSYS Fluent simulation findings had been effectively validated by comparison to the study conducted by Bhinder et al. (2009) It was determined that there was a less than 10% variation in the findings between the simulation and validation source, which is suitable.

This study suggested creating comparable settings to compare the ways in which different buoys behave in waves. Conical, spherical, and odd buoy shapes are taken into consideration. The buoy's motion in the wave is influenced by its size, shape, and wave characteristics. This study investigated how different buoy shapes with constant radius and mass behaved in waves. Contours showed the velocity and pressure around the four buoys. The drag and lift coefficients were intended. The selection of the optimum buoy shape was a complex process that involved several

factors. The primary factors considered in the selection process were the least entropy, maximum lift coefficient and drag coefficient. After careful consideration of the various options, it was determined that the optimum buoy shape was a spherical shape (shape B). This shape was determined to be the best option due to its ability to provide maximum lift and drag coefficients while still maintaining a low entropy value. The results of this study are beneficial in helping to identify optimal buoy shapes for various applications. The lift and drag coefficients are key considerations in determining the buoyancy of an object in a fluid environment such as water. Additionally, the entropy factor is important as it releases how much energy is missing by moving the buoy. By selecting shape B, it was possible to maximize the energy waste and ensure that the buoy would provide an optimal performance.

6. References

- Aderinto, T. and H. Li, (2019). Review on Power Performance and Efficiency of Wave Energy Converters. Energies. 12(22): p. 4329.
- Amiri, A., R. Panahi, and S. Radfar, (2016). Parametric study of two-body floating-point wave absorber. Journal of Marine Science and Application. 15(1): p. 41-49.
- Angeliki Deligianni and Leonidas Drikos, (2023). Floating wave energy harvester: a new perspective, Frontiers in Energy Research, 26 April 2023, DOI 10.3389/fenrg.2023.1122154
- B. Lei, N.Z.W., C. Shang, F. B. Meng, L. K. Ma, X. G. Luo, T. Wu, Z. Sun, Y. Wang, Z. Jiang, B. H. Mao, and Y.J.Y. Z. Liu, Y. B. Zhang, and X. H, (2017). Chen, Tuning phase transitions in FeSe thin flakes by field-effect transistor with solid ion conductor as the gate dielectric.
- Bhinder, M.A., et al., (2009). A Joint Numerical and Experimental Study of a Surging Point Absorbing Wave Energy Converter (WRASPA). p. 869-875.
- C. L. Iandoli, E.S., (2005). 3-D Numerical Calculation of the Local Entropy Generation Rates in a Radial Compressor Stage. International Journal of Thermodynamics, 8.
- De Backer, G., et al., (2010). Bottom slamming on heaving point absorber wave energy devices. Journal of Marine Science and Technology. 15(2): p. 119-130.
- Drew, B., A.R. Plummer, and M.N. Sahinkaya, (2016). A review of wave energy converter technology. Proceedings of the Institution of Mechanical Engineers, Part A: Journal of Power and Energy. 223(8): p. 887-902.
- Falcão, A.F.d.O., (2010). Wave energy utilization: A review of the technologies. Renewable and Sustainable Energy Reviews. 14(3): p. 899-918.
- Falnes, J., A (2007). Review of wave-energy extraction. Marine Structures. 20(4): p. 185-201.
- Finnegan, W. and J. Goggins, (2012). Numerical simulation of linear water waves and wave–structure interaction. Ocean Engineering. 43: p. 23-31.
- George W. Taylor, J.R.B., Sean M. Kammann, William B. Powers, and Thomas R. Welsh, (2001). The Energy Harvesting Eel: A Small Subsurface Ocean/River Power Generator. IEEE JOURNAL OF OCEANIC ENGINEERING.
- Giorgi, G. and J.V. Ringwood, (2016). Computationally efficient nonlinear Froude–Krylov force calculations for heaving axisymmetric wave energy point absorbers. Journal of Ocean Engineering and Marine Energy. 3(1): p. 21-33.

- Gunn, K. and C. Stock-Williams, (2012). Quantifying the global wave power resource. Renewable Energy. 44: p. 296-304.
- Hulme, A (1981). The wave forces acting on a floating hemisphere undergoing forced periodic oscillations.
- Jessica Hernández, Daniel García, Humberto L. Varona, Amilcar E. Calzada, Alejandro Rodriguez, Dailín Reyes, Dayana Carracedo, Ingrid Loaces, Melissa Abreu & Raúl N (2022). Suárez, Wave energy: State of the art and current development, Panamjas; doi.org/10.54451/PanamJAS.17.2.176.
- Kim, M.H., et al., (2001). Fully Nonlinear Multidirectional Waves by a 3-D Viscous Numerical Wave Tank. Journal of Offshore Mechanics and Arctic Engineering. 123(3): p. 124-133.
- Koo, W. and M.-H. Kim, (2011). Freely floating-body simulation by a 2D fully nonlinear numerical wave tank. Ocean Engineering, 2004. 31: p. 2011-2046.
- López, M., F. Taveira-Pinto, and P. Rosa-Santos, (2017). Numerical modelling of the CECO wave energy converter. Renewable Energy. 113: p. 202-210.
- Mahdi Nazari Berenjkoob, M.G., and C. Guedes Soares, (2019). On the improved design of the buoy geometry on a two-body wave energy converter model.
- Malalasekera, H.K.V.a.W., (2007). An Introduction to Computational Fluid Dynamics the Finite Volume Method 2nd Edition. Pearson; (February 6, 2007)
- Mark Z. Jacobson, Mark A. Delucchi, Guillaume Bazouin, Zack A. F. Bauer, Christa C. Heavey, Emma Fisher, Sean B. Morris, Diniana J. Y. Piekutowski, Taylor A. Vencill and Tim W. Yeskoo., (2015). 100% clean and renewable wind, water, and sunlight (WWS) all-sector energy roadmaps for the 50 United States. Energy & Environmental Science. 8(7): p. 2093-2117.
- Ning, D.Z. and B. Teng, (2007). Numerical simulation of fully nonlinear irregular wave tank in three dimensions. International Journal for Numerical Methods in Fluids. 53(12): p. 1847-1862.
- Pastor, J. and Y. Liu, (2014). Frequency and time domain modeling and power output for a heaving point absorber wave energy converter. International Journal of Energy and Environmental Engineering. 5(2-3).
- Shehata, A.S., et al., (2016). Performance analysis of wells turbine blades using the entropy generation minimization method. Renewable Energy. 86: p. 1123-1133.
- Sun, H. and O.M. Faltinsen, Water impact of horizontal circular cylinders and cylindrical shells. Applied Ocean Research, 2006. 28(5): p. 299-311.
- U. G.X.W.u.a.n.d.Z.Z.H., (2004). Simulation of nonlinear interactions between waves and floating bodies through afinite-element-based numerical tank.
- Viet, N.V., et al., (2016). Energy harvesting from ocean waves by a floating energy harvester. Energy. 112: p. 1219-1226.
- Yan, H. and Y. Liu, (2011). An efficient high-order boundary element method for nonlinear wave–wave and wave-body interactions. Journal of Computational Physics. 230: p. 402-424.